Asian Journal of Pharmaceutical Sciences 16 (2021) 265–279

Available online at www.sciencedirect.com

ScienceDirect

journal homepage: www.elsevier.com/locate/AJPS

Review

The application of label-free imaging technologies in transdermal research for deeper mechanism revealing

Danping Zhang[a], *Qiong Bian*[a], *Yi Zhou*[a], *Qiaoling Huang*[b], *Jianqing Gao*[a,c,*]

[a] *Institute of Pharmaceutics, College of Pharmaceutical Sciences, Zhejiang University, Hangzhou 310058, China*
[b] *The Third People's Hospital of Hangzhou, Hangzhou 310012, China*
[c] *Jiangsu Engineering Research Center for New-Type External and Transdermal Preparations, Changzhou 213000, China*

ARTICLE INFO

Article history:
Received 20 March 2020
Revised 23 May 2020
Accepted 6 July 2020
Available online 24 August 2020

Keywords:
Infrared spectroscopy
Raman spectrum
Mass spectrometry
Label-free imaging technology
Mechanism research

ABSTRACT

The penetration behavior of topical substances in the skin not only relates to the transdermal delivery efficiency but also involves the safety and therapeutic effect of topical products, such as sunscreen and hair growth products. Researchers have tried to illustrate the transdermal process with diversified theories and technologies. Directly observing the distribution of topical substances on skin by characteristic imaging is the most convincing approach. Unfortunately, fluorescence labeling imaging, which is commonly used in biochemical research, is limited for transdermal research for most topical substances with a molecular mass less than 500 Da. Label-free imaging technologies possess the advantages of not requiring any macromolecular dyes, no tissue destruction and an extensive substance detection capability, which has enabled rapid development of such technologies in recent years and their introduction to biological tissue analysis, such as skin samples. Through the specific identification of topical substances and endogenous tissue components, label-free imaging technologies can provide abundant tissue distribution information, enrich theoretical and practical guidance for transdermal drug delivery systems. In this review, we expound the mechanisms and applications of the most popular label-free imaging technologies in transdermal research at present, compare their advantages and disadvantages, and forecast development prospects.

1. Introduction

The transdermal drug delivery system (TDDS) is an important drug delivery strategy, which is particularly suitable for the drugs that show serious adverse reactions when administered orally, drugs acting on skin or local subcutaneous tissue or drugs that are more effective when administered by transdermal delivery, etc. Skin is the delivery pathway for topical substances and plays a role for barrier function.

* Corresponding author.
E-mail address: gaojianqing@zju.edu.cn (J.Q. Gao).
Peer review under responsibility of Shenyang Pharmaceutical University.

https://doi.org/10.1016/j.ajps.2020.07.004

The molecular weight, aqueous solubility, lipid solubility, permeability coefficient and octanol-water partition coefficient are considered to influence the penetration, distribution and transport of topical substances in skin. In the traditional way, the *in vitro* permeability of substances in skin can just be compared by measuring their concentration in the Franz diffusion cell receiving solution by high-performance liquid chromatography (HPLC). Tape strapping can be further exerted to separate the stratum corneum (SC) from intact skin and quantify the retention amount for a substance in the SC, which is the main barrier for skin. However, this quantitative method would lead to the loss of most of the spatial distribution information [1,2], and cannot be used to reflect the whole percutaneous process.

More accurate and abundant experimental data, especially the data containing spatial distribution information, are important. On the one hand, for reducing repeat experiments and following the banning of animal testing for cosmetics, in silicon dynamics simulation and mathematical prediction can be a good alternative. The establishment of a mathematical model to screen suitable transdermal drugs or assess skin toxicity strongly relies on detailed experimental data. Actually, predictive mathematical models, including quantitative structure permeability relationships (QSPR) model and dynamics simulation, based on traditional experimental data usually show bias when comparing with practical consequences [3]. To increase the accuracy of the prediction obtained from mathematical models, the dynamic distribution of topical substances in the hydrophilic or lipophilic domains and appendages should be taken into account.

On the other hand, the absorption, distribution, metabolism and transport of topical substances are essential parts of pharmacology and toxicology research. Tracking the disposal of topical substances in skin is sometimes necessary, especially when considering skin irritation and skin therapeutic effects, such as for sunscreen and hair growth products. The effect of penetration enhancers can also be revealed by characteristic imaging. Exposing the penetration pathway and the distribution of topical drugs in the presence of penetration enhancers will greatly help transdermal research and formulation development.

The functions of a skin barrier will be influenced by environmental factors, such as hydration and heating, artificial interventions and some chemicals. Penetration enhancers are commonly used to promote the transdermal transport rate of topical agents [4-6], for which possible mechanisms mainly include: (1) altering the skin physiological state; (2) destruction of SC barrier function; (3) changing the physical and chemical properties of the substance, etc. [7-9]. Based on these hypotheses, attenuated total reflection-fourier transform infrared, Raman spectroscopy, differential scanning calorimetry, X-ray scattering and ^{1}H NMR have been applied to reveal the configuration changes of skin SC lipids and proteins caused by penetration enhancers [10]. However, it is hard to give an exact answer when the following questions are involved. How does the increased amount of topical substance transport through the skin? Does such transport occur through intercellular, intracellular or skin appendages? Do the penetration enhancers penetrate into the deep skin accompanied by the drugs? Directly imaging the transdermal substances will help us to answer these questions.

The first method that comes into mind might be fluorescent dye labeling. Fluorescent dye labeling is able to track the dynamic process of substances in tissues with high image resolution. However, the molecular mass of fluorescent tags is usually much higher than that of topical agents (mostly less than 500 Da). Fluorescent dye labeling can inevitably change the dynamic behavior of target substances. Optoacoustic imaging, optical coherence tomography, high-frequency ultrasound imaging and terahertz imaging possess the ability to illustrate the skin morphology structure and distinguish pathological tissue, but without the ability of characteristically analyzing compounds.

Based on these reasons, a characteristic, high-resolution and label-free imaging technology has been strongly demanded to cater for the requirement of exploring the transdermal enhancing mechanism and revealing the interaction between topical substances and skin. At present, researchers have developed some technologies for skin label-free imaging based on the unique characteristics of the substance involved, such as measurement of the vibration spectrum and molecular mass. These technologies cannot only be used for the imaging of SC tapes and skin sections, but can also be applied onto intact skin and even used for *in vivo* detection, as shown in Fig. 1. In this review, we introduce some of the most commonly used label-free imaging technologies (Fig. 2), briefly describe their imaging principles, expound the current progress for research into the transdermal mechanism, and compare the advantages and disadvantages of these technologies.

2. The structure of skin and the penetration theory

Skin is a complex multifunctional organ composed of epidermis and dermis, with various functional appendages [11,12]. SC, the outmost layer of skin, is considered to be the main barrier to obstruct exogenous substances from entering skin. SC is composed of 10–20 layers of dead flat corneocytes, which are rich in α-keratin filaments [13,14] and coated by well-organized intercellular lipids and proteins [15,16]. The dense lipophilic intercellular matrix plays a decisive role when substances pass through SC [17-19]. Compared with SC, the active epidermis and dermis contain a high amount of water. Cell differentiation and migration of the active epidermis lead to regular replacement of the SC. The dermis layer is rich in collagen and reticular fibers [15,20], and embedded with extensive blood vessels, lymphatics, hair follicles, nerve endings and glands. Therefore, the dermis allows a drug to be exchanged and enter systemic circulation [21]. Due to the barrier function and specific physiological structure of skin, only a small number of external substances can enter systemic circulation, with some substances deterred or trapped in the skin.

The penetration and transport dynamics of topical substances closely related to the structural characteristics of

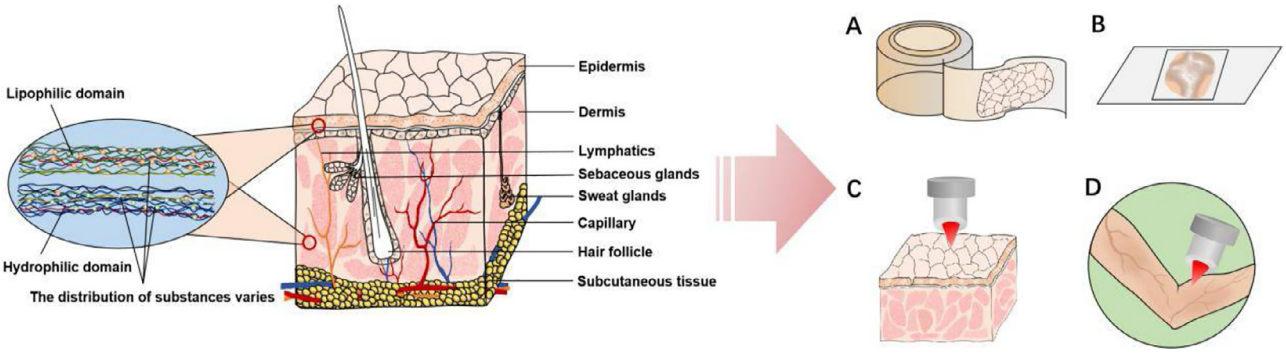

Fig. 1 – Investigating skin by label-free imaging technologies can be performed by tape stripping (A), tissue sections (B), or directly carried on intact skin *in vitro* (C) or *in vivo* (D).

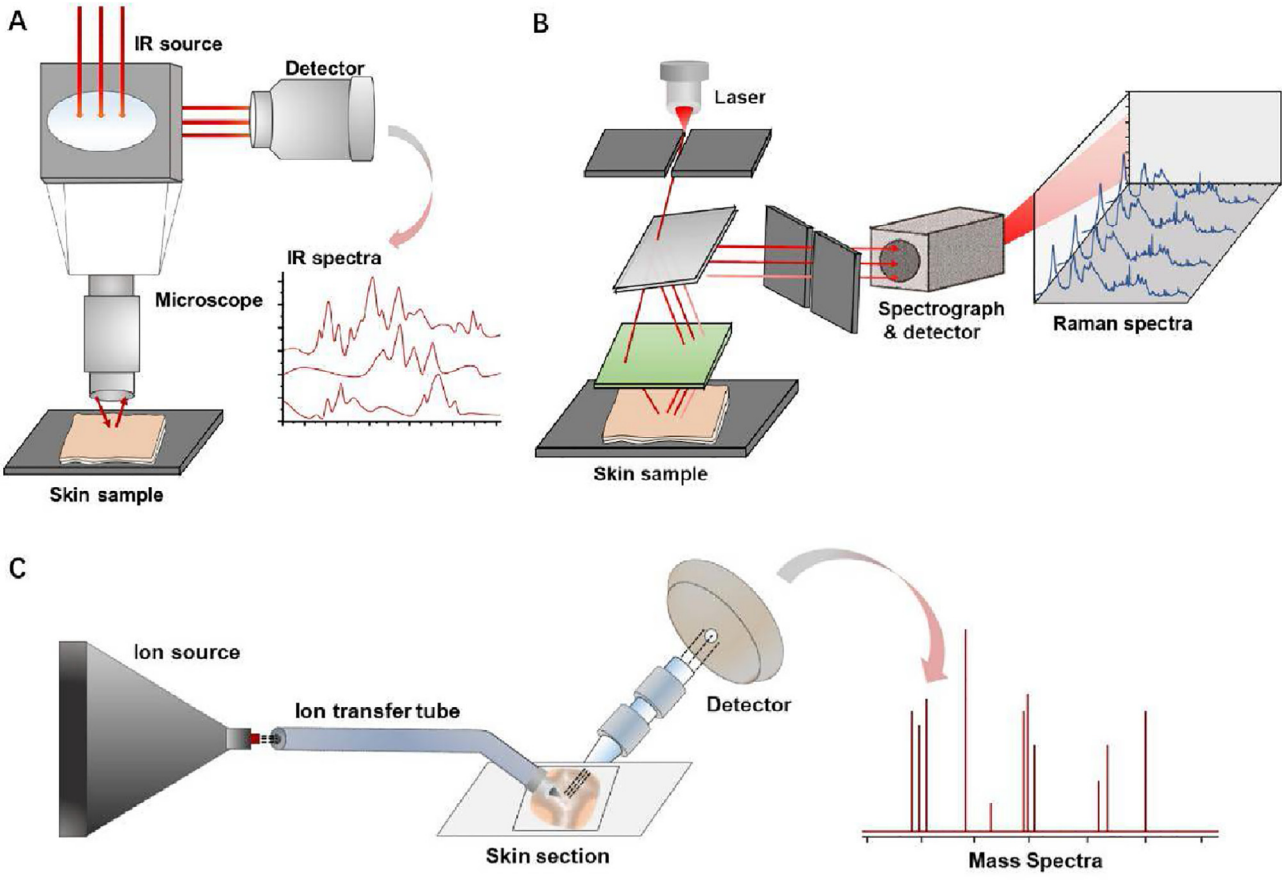

Fig. 2 – Infrared spectroscopy (A), Raman spectrum (B) and mass spectrometry imaging (C) can distinguish the target substances from the complex skin background according to the characteristic vibration signals or mass-to-charge ratio (*m/z*).

skin. Compounds show significant distribution differences in skin's lipophilic part and hydrophilic part. Blood, lymphatic or capillaries transport, and protein binding determine the dermal transport of compounds, which may also relate with the chemical configuration and physicochemical properties [22]. Accordingly, mathematical models of skin penetration and transport simulate the heterogeneity of the skin by dividing it into the multiple sub-layers or compartments. The diffusion in individual cell is usually described by Fick's first law. The transference from one compartment to another could represent by a set of first-order rate constant [23]. For example, Laplace transform was employed as mathematical tool for finding the solution of skin diffusion equation [24]. However, a more practical mathematical model needs to take numerous factors into account, especially in the epidermal and dermal transport.

3. Label-free imaging technologies

3.1. *Infrared spectroscopy*

Compounds with characteristic vibrational spectra can be distinguished from complex biological backgrounds according to spectra-structure correlations, which enables wide use of infrared spectroscopy and Raman spectroscopy in biochemical research. Infrared (IR) spectroscopy has been applied to skin analysis and imaging for several decades, which measures characteristic absorbance or attenuated reflectance of light in different frequency range of the samples. Molecules with active IR vibration group, which do not overlap with endogenous skin IR spectrum can be recognized and analyzed by IR imaging. When employed in analyzing an intact skin, Fourier transform infrared (FTIR) spectrum usually represents the average signal of the area that the light passed through. When combined with array detectors, such as commonly used focal plane array detector, FTIR will take chemical resolution information and spatial imaging of multicomponent samples [25]. Attenuated total reflection (ATR)-FTIR spectroscopy combined with ATR accessory can reach much higher sensitivity, in which incident light produced by light source travels across a crystal with high refractive index and totally internal reflects after contacting with samples' surface. Therefore, skin samples need to be tightly compacted on the surface of ATR crystal to avoid the interference of air. ATR-FTIR spectroscopy can be used for tissue imaging and obtaining qualitative structure information and semiquantitative analysis [26,27].

3.2. *Raman spectroscopy*

Raman spectroscopy is a detection and imaging technology, which is based on the Raman effect, as first observed by Raman CV in 1928. When a beam of light strikes an object, elastic scattering and inelastic scattering occur. The scattering spectra are divided into Rayleigh scattering and Raman scattering according to the energy change and wavelength shift. Rayleigh scattering spectra show the same wavelength as the incident light. In contrast, Raman scattering spectra show different wavelengths, the scattering with longer wavelengths and lower energy called Stokes scattering, and the scattering with shorter wavelengths and higher energy called anti-Stokes scattering. Raman microscopes can be used for qualitative and quantitative detection by analyzing specific wavelength migration, thus, such a technique does not need labeling tags as required by a fluorescence microscope. Because of the characteristic Raman spectra for chemicals and the linear relationship between scattering intensity and excitation of functional groups, Raman microscopy is regarded as a proper tool to explore the fate of compounds in intact biological tissues.

Spontaneous Raman scattering signal is so weak (only one of 10^8 photons occurs Raman scattering) [2] that the acquisition process usually takes several hours, especially in the panoramic scanning of large biological samples, which is improbable to obtain high-resolution 3D imaging or track the dynamics processes for chemicals. Stimulated Raman scattering microscopy (SRS), coherent anti-Stokes Raman scattering microscopy (CARS) and surface-enhanced Raman scattering (SERS) have been developed based on the Raman effect. SERS was discovered in the 1970s, in which the Raman scattering intensity on rough surfaces such as silver, gold and copper is greatly enhanced [28]. Therefore, a stronger Raman scattering signal can be obtained. Because of the dependence on rough metal surfaces, SERS is generally used for the detection of metal nanoparticles or devices with a metal coating.

Coherent Raman scattering (CRS) breaks through the limit of detection speed, and greatly increases the intensity of the Raman signal measured while achieving rapid image acquisition and submicron resolution. CARS and SRS are two main types of coherent Raman scattering. CARS involves a four-wave mixing nonlinear optical process, in which the vibration group of Raman active molecules interacts with the incident light field, which leads to a vibration transition from the ground state to excited state. When the pump beam and Stokes beam overlap in a medium, they will coherently excite vibration or rotation of molecules. The coherent excitation of vibration or rotation will mix with the incident light field again, following which four coherent Raman scattering signals appear simultaneously. However, during the CARS process, the nonresonant background effect cannot be ignored, which limits the detection sensitivity and distorts the obtained CARS spectra. The nonresonant background originates from the four-wave mixing process interacting with the field where no resonant molecules are present [29,30]. Accordingly, researchers have tried to eliminate the nonresonant background as much as possible through improvement of equipment and mathematical models [31-33]. The reported hardware-based approaches included time-resolved CARS, polarization CARS, and λ-switch scheme [34], which image sequentially target compounds and nonresonant background, etc. Mathematical approaches such as maximum entropy algorithm suppressing non-resonant background by identifying the imaginary component of the anti-Stokes field [35]. But these alternative approaches might leaving higher requirements for researchers.

Stimulated Raman scattering (SRS) relies on the strong interaction between high intensity laser and targeted molecules. SRS employs a pump beam and Stokes beam, which are spatially and temporally synchronized picosecond laser pulse trains [36,37]. The energy gap between these two lasers can be adjusted to match the vibration of the targeted chemical bonds. When the two beams are directed onto samples, the intensity transfers from the pump beam to the Stokes beam and stimulates excitation of Raman active molecular vibrations [38,39]. The detecting module usually modulates the Stokes beam and detects the change of pump beam intensity using a photodiode and lock-in amplifier.

Unlike CRAS, the SRS signal is linearly proportional to concentration, so a quantitative analysis can be carried out without complicated calculation. Moreover, SRS is free of a nonresonant background and has no obvious interference from spurious signals. SRS offers higher spatial resolution, significantly improved scan speed, and an orders of magnitude greater sensitivity compared to spontaneous

Raman scattering [40,41]. Moreover, researchers have been constantly improving the SRS device to overcome its defects or meet the requirement of different experimental conditions. Fu et al. [42] presented a novel modulation multiplexing approach that allowed multispecies chemical mapping. Three channels of this multiplex SRS could be used to separate pigment absorption, lipids SRS and protein SRS, and disentangle the major biochemical composition of different skin layers with a speed that was at least three orders of magnitude faster than that achieved by confocal Raman imaging.

3.3. *Mass spectrometry imaging*

Mass spectrometry imaging (MSI) technology, which originated in the 1970s, has developed rapidly in the past few decades owing to its high specificity and sensitivity. In recent years, researchers have introduced MSI into the study of transdermal transport of topical substances. MSI can be used to simultaneously image the distribution of endogenous and exogenous compounds, including lipids, proteins, drugs and metabolites, without the use of fluorescent labeling or radiolabeled compounds. The specific mass spectrum allows MSI to accurately distinguish and image numerous compounds, enabling MSI to be widely used in drug detection, pharmacokinetic analysis, histopathological characterization and metabolomic tracking in kidney, heart, lung, brain, tumor, skin and so on.

Secondary-ion mass spectrometry (SIMS) is used to obtain *m/z* signals by bombarding the surface of samples with a high energy pulsed primary ion beam. The sample surface absorbs energy and sputters secondary ions, which are then collected by a mass analyzer. Time of flight secondary-ion mass spectrometry (ToF-SIMS), one of the most commonly used SIMS, separates signals through the flight time of secondary ions in the mass spectrometer, and draws maps by scanning sample surfaces with a focused ion beam. Improved SIMS replaces high-energy primary ions (usually Ga^+, $^{133}Cs^+$, Au_3^+, Bi_3^+, Bi_5^+, $^{40}Ar^+$, C_{60}^+, etc.) with softer ions [43-45] and updates the equipment design. Water-containing cluster beams have been reported to increase the secondary-ion yield and enhance the spatial resolution to ≤ 1 μm. Mohammadi et al. [46] demonstrated that a high-energy (40 keV) gas cluster ion beam allowed one to obtain more intact lipid compound signals in mouse brain, which acted similar to semisoft ionization.

Matrix-assisted laser desorption ionization (MALDI) is the most widely used MSI method at present. By pretreating with a radiation-absorbing matrix, which cocrystallizes with analytes and transfers absorbed energy to the lower layer, one can avoid strong molecular damage caused by direct ion collisions. It was reported that MALDI-MSI provides a large molecular mass range (up to 80 kDa [47,48]) and high spatial resolution in the biological imaging of proteins, lipids and other macromolecules. The choice of matrix and the pretreating process exert an essential influence on the imaging quality of MALDI-MSI. Uniformity of the matrix coverage, size of the matrix crystals and diffusion of the analyte in the solvent directly impacts the imaging spatial resolution and accuracy [49-51]. The matrix should be chemically stable, and should form a uniform matrix coating, besides showing a good ionization ability for target substances. For MALDI-MSI, 2,5-dihydroxybenzoic acid, 9-aminoacridine, α-Cyano-4-hydroxycinnamic acid, 4-phenyl-α-cyanocinnamic acid amide, 1,5-diaminonaphthalene, N-(1-naphthyl) ethylenediamine dihydrochloride, etc., have been constantly used in sample preparation. However, for different target substances, these matrices may present different imaging effects, which is why many studies have focused on finding a more suitable matrix. In addition, in the imaging of small molecular substances with a molecular mass less than 1000 Da, matrix selection is necessary to minimize the signal interference from the matrix. Therefore, some new matrices have been explored to obtain better imaging results on certain tissues or molecules. For example, curcumin was reported to have been used to successfully image acitretin, lipids, peptides, and proteins in skin and lung [52]. For the pretreating process, modifying the glass slide surface with corona discharge was reported to improve the adhesion of skin tissue sections [53]. Washing samples with acetone [54] or chloroform [55] was considered to reduce the interference of matrix-related ions and ionization-suppressing effect.

A high-vacuum environment or complex sample pretreating process makes it impossible to carry out some operations that need to be carried out under ambient conditions. Unlike SIMS and MALDI-MSI, the ambient ionization method is a newly developed soft ionization approach operated under atmospheric pressure. The combination of desorption electrospray ionization (DESI) with MSI is the most common atmospheric mass spectrometry, in which charged microdroplets are sprayed directly onto tissue, followed by dissolution and desorption of the analyte into the detecting system, via which the noninvasive and *in vivo* analysis of samples becomes available.

Other mass spectrometry imaging technology, such as liquid extraction surface analysis (LESA) mass spectrometry, laser ablation electrospray ionization (LAESI) mass spectrometry, laser desorption postionization (LDPI) mass spectrometry and femtosecond laser desorption postionization mass spectrometry (fs-LDPI-MS) have also been acknowledged as powerful tools for detecting and imaging lipids, proteins, metabolites and drugs in tissues samples, but which have been rarely introduced into transdermal research.

4. The application of label-free imaging technologies

4.1. *The application of infrared spectroscopy*

The images or spectra obtained by IR spectroscopy can be roughly used to distinguish the spatial distribution of topical agents in different skin section layers. In addition, the quantitative ability of IR spectroscopy can further help to reveal penetration kinetics, though not accurately enough. According to reports, changes in the characteristic absorption peak intensity for topical agents, such as Emu oil [56], perdeuterated oleic acid [57], dimethyl sulfoxide [58], caffeine [59], propylene glycol [60] and ethanol

[61], with depth, diffusion time, lipophilic domains or skin physiological conditions in skin section have been successfully converted into images by IR spectroscopy. For example, the lateral distribution of acyl chain perdeuterated oleic acid and deuterated dimethyl sulfoxide in human stratum corneum with diffusion time were tracked from changes in CD_2 (~2100 cm^{-1}) and Amide I stretching frequencies (~1626 cm^{-1}) [57]. The characteristic absorption band of Emu oil at 3006 cm^{-1}, where is free of skin endogenous IR spectra, helped representing it's penetration in human skin section [56].

However, these studies often indicated that the discrimination ability of the IR spectrum might not be credible enough, because skin is a complex system, and many substances show overlapping infrared absorption peaks. Furthermore, it is worth mentioning that quantitative analysis is realizable without deuteriation by tracking the characteristic vibration peak of a target compound, or subtracting spectra obtained for untreated skin samples from those obtained for treated skin samples. Nonetheless, due to the interference of skin background signals, deuteriation, which will shift target stretching frequencies to a spectral region free of interference from skin background vibrations, is usually necessary to better distinguish a targeted spectrum or differentiate substances with similar structures.

Intact skin detection is more convenient for sample preparation, as well as for maintaining sample integrity and decreasing data distortion. The penetration depth of infrared light in biological tissues is usually limited to only 1–2 μm; this is why tape stripping is usually performed first before ATR-FTIR when analyzing intact skin samples [62,63]. SC can be peeled off by tape stripping for several times, followed by quantification and imaging by ATR-FTIR. The differences detected between different stripping times reveal the distribution of substances in the vertical layer of the SC. ATR-FTIR combined with tape stripping has been reported to be used to monitor or image the distribution of flufenamic acid [64], diclofenac sodium [65], sodium lauryl ether sulfate [66], sodium dodecyl sulfate [62], phospholipids [67], sucrose laurate [68], 4-undecanolide [26], and chitosan [69], etc. For example, Andanson et al. measured the diffusion of benzyl nicotinate and ethanol through the outer layer of human skin *in situ* and revealed the correlation between the distribution of SC lipids and drugs [63]. Cozzi et al. evaluated and compared the retention and penetration of sunscreen formulation inside the skin by sequential tape strips and FTIR. The skin before and after tape stripping was observed by FTIR, in which the skin deposition in vertical SC layers provoked by different sunscreens could be differentiated [70]. Because of the noninvasive experimental process involved, tape stripping is also frequently applied onto human skin *in vivo*, and FTIR is accompanied for qualitative and quantitative study [71,72]. Tape stripping carried out *in vivo* will objectively reflect the pharmacokinetics of drugs in the SC.

In addition, ATR-FTIR is also a typical method used in skin structure changes revealing. The lipophilic and hydrophilic domains of skin mainly composed of lipids and proteins are usually distinguished based on the characteristic absorption spectrum [73]. The configuration changes in proteins and lipids as revealed by ATR-FTIR are considered as meaningful evidence for the influence of exogenous substances, especially penetration enhancers. In clinical diagnosis, the intensity change and shift of characteristic absorption bands can indicate pathological progress in skin.

4.2. *The application of Raman spectroscopy*

Confocal Raman microscopy (CRM) has been widely used in tracking the penetration process of topical drugs, penetration enhancers, pharmaceutical excipient, cosmetic ingredients and environmental substances, such as sodium dodecyl sulfate [74], metronidazole [75], trans-cinnamaldehyde [76], hyaluronic acids [77], retinol [78], and oils [79], in excised human skin, porcine skin or reconstructed human skin models. Mujica Ascencio et al. [80] used CRM to simultaneously determine the penetration abilities of caffeine and propylene glycol in *ex vivo* porcine skin at different excitation wavelengths (633 nm and 785 nm), and multivariate statistical methods were employed to calculate their penetration depths. Pyatski et al. [81] employed flufenamic acid as a model drug to investigate the enhancing effect of hydrophobic enhancer, octanol, *versus* hydrophilic enhancer, propylene glycol/ethanol (75/25), and obtained the relative concentrations and images of colocation spatial distribution for both the enhancers and flufenamic acid in *ex vivo* human skin. Bakonyi et al. [82] drew the spatial distribution of lidocaine and tracked the penetration of the drug from different carriers in *ex vivo* human skin. The essay published by Darvin et al. showed that an immune response modifier, TMX-202, can reach langerhans cells through intercellular, transcellular, and follicular pathways [83]. CRM also exhibits the ability of distinguishing endogenous chemicals and picturing skin appendage, including sebum, follicle and glands [84].

Raman spectroscopy is also a prevailing method for *in vivo* detection. Raman spectroscopy is able to monitor the diffusion behavior of topical drugs and cosmetics, especially those showing skin toxicity, irritation or a skin pharmacological effect. Thus, the safety and efficacy of these products, which have roused much attention, can be further revealed. According to reports, Mélot et al. have monitored the effect of penetration enhancers on the ingress of trans-retinol into skin by *in vivo* CRM [85]. Laing et al. concluded that a paraffin petrolatum-based product would remain in the SC based on *in vivo* imaging for Caucasian volunteers [86]. Retinyl acetate was detected at different forearm skin depths of up to 20 μm, 30 min after administration [87]. The skin depth distribution for skin care products such as urea [88], sunscreens [89] could also be obtained by *in vivo* CRM. Compared with IR spectroscopy, Raman spectroscopy has an ability to generate a deeper penetration depth and higher resolution, which can be used to clearly distinguish skin layers and structures, and present more skin details.

Compared with CRM, CRS can be used to provide higher spatial resolution and richer structure information. According to recent reports, CARS can be often combined with two-photon microscopy to simultaneously obtain the substance distribution information and skin morphology information. Combining CARS with two-photon excited native fluorescence, Chen et al. [20] detected the penetration

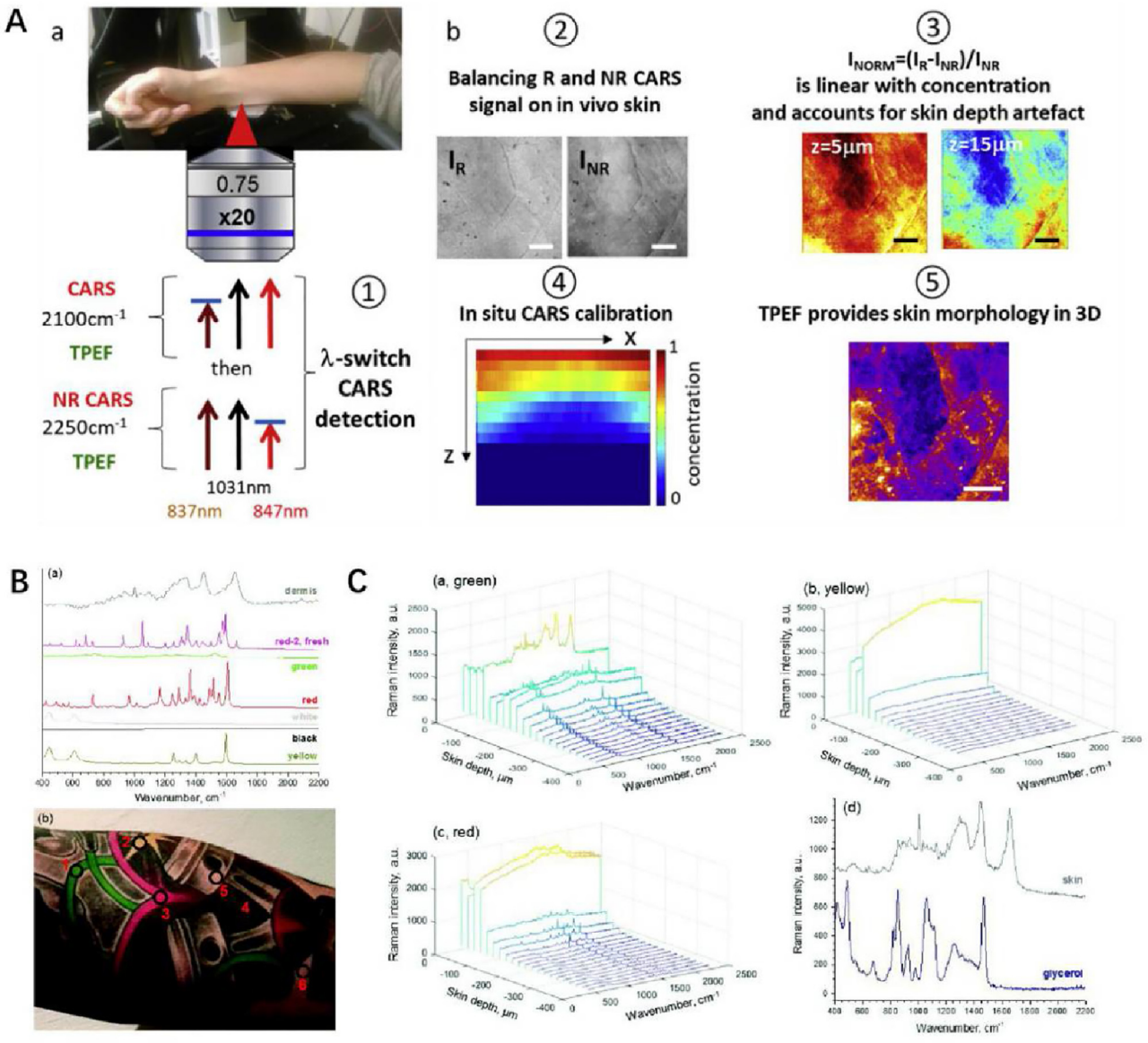

Fig. 3 – Raman spectroscopy could be used for *in vivo* detection with gratifying results. (A): The designed CARS and two-photon autofluorescence imaging system successfully quantified the percutaneous penetration *in vivo* of deuterated glycerol diluted in water and xanthan gel. (Reproduced with permission from [34], Copyright 2019 Elsevier B.V.). (B&C): The Raman spectra obtained after treatment by optical clearing agent glycerol showed a significant enhancement of the investigated depths of tattoo on the inner forearm, from ≈75 μm down to 400 μm. (Reproduced from [105], Copyright 2018 The Royal Society of Chemistry).

pathway and calculated the normalized concentration of deuterated glycerol, deuterated synthetic jasmonic acid derivative and heavy water in reconstructed skin and excised human skin. Sarri et al. [34] from the same group, imaged and quantified deuterated glycerol penetrating into human skin *in vivo* using the combination technology. With the morphology information provided by two-photon excited native fluorescence, 3D quantitative active compound mapping can be merged with detailed morphological identification (as shown in Fig. 3A-b⑤). In addition, the introduction of λ-switch was said to increase sensitivity and correct the beams scattering and excitation with increasing skin depth (Fig. 3A-a), which schemed to image sequentially deuterated molecular compounds (2100 cm^{-1}) and CARS non resonant background (2250 cm^{-1}) (Fig. 3A-b③④), and enabled to build liner-relationship between signal with concentration (as shown in Fig. 3A-b②).

Compared with CARS, there have been more reports on the molecular mechanism at the cellular level carried out with SRS at a satisfied resolution of up to 130 nm [90]. In addition, researchers have also introduced SRS into the study of the transdermal mechanism based on its excellent imaging ability. Guy's group directly observed ibuprofen and ketoprofen penetrating through the SC and hair follicles based

on the high-speed three-dimensional imaging capability of SRS [91]. They also visualized the formation of ibuprofen and ketoprofen crystals on a porcine skin surface and semi-quantified the penetration amount [92]. Drutis et al. [93] accurately imaged the three-dimensional structure of skin, demonstrating the presence of corneocytes clusters and canyon in the SC, as well as illustrating the distribution of topical oleic acid-d_{34} in these structures. Garrett et al. [94] mapped the distribution of antifungal compounds, zinc pyrithione and climbazole, in interfollicular epidermis and infundibular space surrounding hair shafts with cellular precision. In this way, its pharmacological effects can be related to transdermal efficiency and skin distribution. Although SRS has been more commonly used in biochemical research in most published studies, such as for observing the change in tissue composition with growth time, and the synthesis and metabolism of intracellular DNA and protein, its powerful imaging ability and good substance discrimination makes us believe that SRS will attract interest from more researchers who are interested in the study of the transdermal mechanism.

Raman data analysis is complex, especially in transdermal research, for the interference of inhomogeneous background signal, which covering the entire spectrum, and the dissipation of laser beam in the deep tissue. In order to identify and classify the target spectra, multivariate curve resolution and K-means clustering analysis are mostly employed. They can extract the pure spectrum or classify similar spectra in groups, respectively [95]. For further quantitative analysis and penetration kinetics fitting, mathematical models, such as classical least squares model [96] and non-negative constrained least squares analysis [97] showed the ability to convert Raman data into concentration information. The refraction and dissipation of the Raman signal in the deep the skin cause the serious data distortion. The introduction of internal reference is an effective solution. For example, Franzen et al. [98] used unspecific methyl deformation vibration in the wavenumber range of 1388–1497 cm^{-1} as an endogenous internal reference for model drug caffeine quantitative depth profiling in skin. Alonso et al. [99] correlated the caffeine peak using the aromatic amino acid and amide I peak. The keratin peak at a wavenumber of approximately 1650 cm^{-1} has also been commonly used as a normalized peak [100]. Although still not sufficiently precise, these correction methods have provided a good reference for revealing the transdermal dynamics of topical substances.

Photobleaching has been reported to reduce the autofluorescence of skin and enhance the intensity of the Raman signal. The fluorescent components in skin, including phospholipids, keratin, vitamins, porphyrins, melanin, etc., emit autofluorescence in the near-infrared, ultraviolet and visible light regions [101,102]. The phenomenon of decreased autofluorescence intensity upon light irradiation is called photobleaching. However, few relevant studies have been adopted that utilize the photobleaching effect to improve the signal-to-noise ratio and increase the penetration depth of light for Raman spectroscopy [103,104].

Optical clearing is another method that has been used to increase the intensity of the Raman signal. As reported by many researchers, the application of optical clearing agents can effectively decrease the absorption and scattering of light in biological tissues, thereby greatly increasing the penetration depth of optical microscopes. Glycerol is a widely reported light scavenger. In a *in vivo* study, the deposition of different tattoo ink in human papillary was detected by Raman microspectroscopy (as shown in Fig. 3B). Topical application of glycerol combined with tape stripping has been used to successfully increase the obtained Raman spectra from 40 μm to 400 μm (Fig. 3C) [105]. Sorbitol [106], hyaluronic acid [106], dimethyl sulfoxide [107] have also been shown to have significant light clearing effects on skin samples. Sdobnov et al. [108] employed an approved pharmaceutic substance, Omnipaque™, as a novel optical clearing agent, which showed a lower optical clearing effect but with higher safety and more promising application value compared with glycerol. The specific mechanism involved in the optical clearing process is still under discussion. The prevailing consensus considers that the modification of the scattering properties of tissues might originate from the dissociation of collagen fibril and the cell dehydration caused by the difference in the biological membrane permeability between optical clearing agents and water [109-111].

4.3. *The application of mass spectrometry imaging*

MSI can be used to image not only macromolecular substances but also small molecular substances. MSI has been widely reported to be used in the imaging of lipids, proteins, etc., and can be used to track metabolic changes, component evolution in diseases or the maturation of tissues and organs. The powerful multisubstance imaging capability of MSI makes it a promising label-free imaging technology. TOF-SIMS has been reported to be used to locate and image chlorhexidine digluconate [112], TiO2 [113], fatty Acid [114], vitamin C [115], lidocaine [116] and imiquimod [117] in skin, and for describing the permeation behavior of these topical agents or comparing the effect of penetration enhancers. After SIMS detection, tissue samples can be further observed by scanning electron microscope (SEM) to acquire morphological information. Combining TOF-SIMS and SEM, Sjövall et al. [118] synchronously obtained the morphological structure of mouse ear skin and topical drug location in different skin layers. In addition, the results indicated that roflumilast, tofacitinib, and ruxolitinib are mostly located in the SC (Fig. 4A). This combined method was also used to image the spatial distribution of endogenous skin components, including ceramide, saturated long-chain fatty acids, and cholesterol sulfate from the SC down to the dermis in excised human abdominal skin [119].

MALDI-MSI is more widely used, and has been reported to be successfully employed in the analysis of excised human skin, artificial model skin, and porcine skin, as well as for simultaneously comparing the absorption capacity of topical agents. The reported drugs include roflumilast [120], tofacitinib [120], bleomycin [121], imipramine [122], acetretin [123], ketoconazole [124], etc. Marxen et al. [125] assessed the impact of chemical permeation enhancers, such as sodium taurodeoxycholate, dimethyl sulfoxide, sodium dodecyl sulfate and azone on the permeability of [^{3}H]-nicotine and

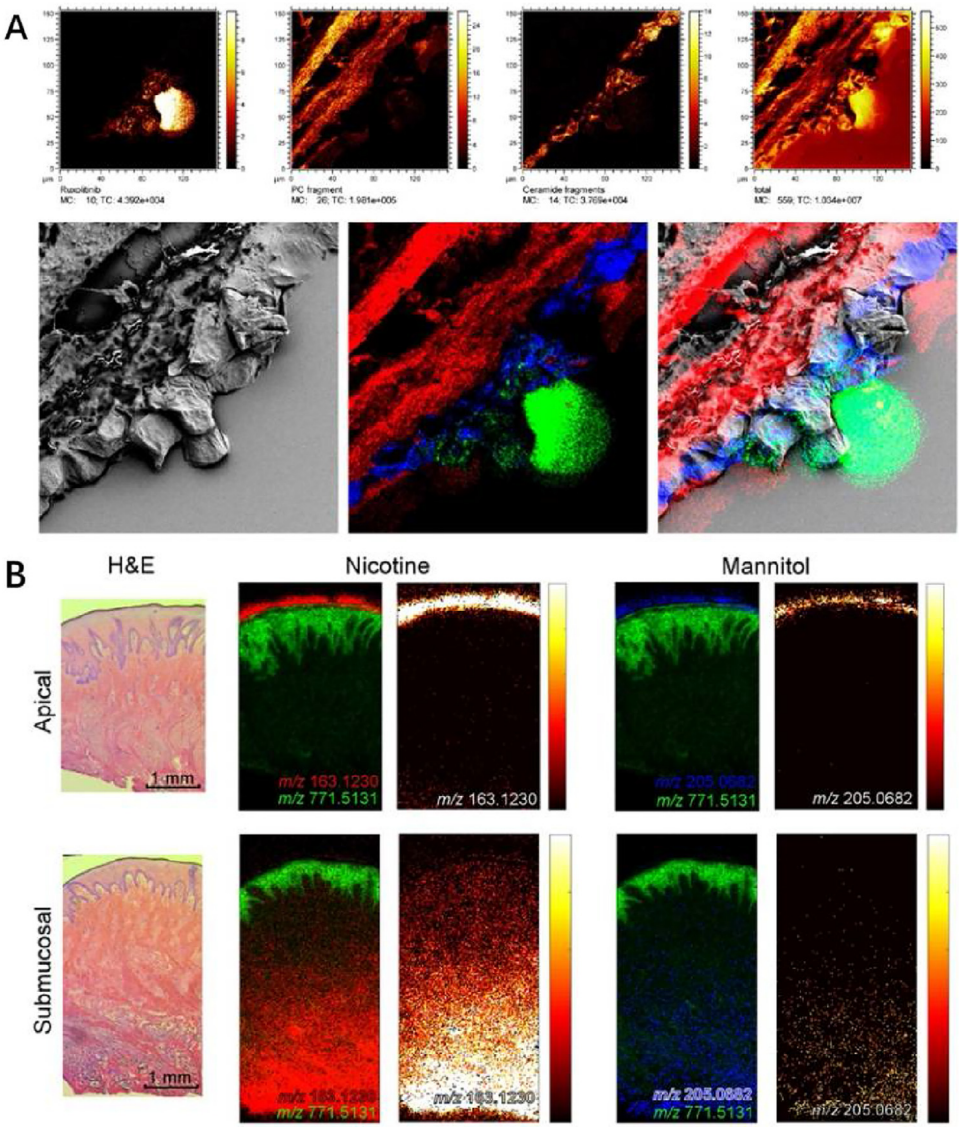

Fig. 4 – MSI imaging could combined with morphological observations, such as SEM and H&E staining. (A): A previous work used TOF-SIMS to co-locate ruxolitinib (green), phosphatidylcholine (PC) fragments (red) and ceramide fragment (blue) in mouse ear. SEM imaging was carried out after TOF-SIMS to identify the different skin layers. (Reprinted with permission from [118], Copyright 2014 American Chemical Society). (B): H&E staining and MALDI-MSI were applied on a cross section of porcine buccal mucosa exposed to nicotine and mannitol solution. Red: Nicotine. Blue: Mannitol. Green: Epithelial marker. (Reprinted with permission from [126], Copyright 2017 American Chemical Society).

mannitol across porcine buccal mucosa by imaging all of these compounds by MALDI-MSI, as shown in Fig. 4B. The spatial resolution of nicotine and mannitol reached 10 μm or even higher [126]. In another study, the spatial distribution of caffeine and mannitol with or without sodium dodecyl sulfate in porcine buccal mucosa was analyzed by MALDI-MSI. The spatial distribution result indicated that sodium dodecyl sulfate had permeated into one-third of the epithelium, with the permeability increase of mannitol in the outer part of the epithelium, which comfirmed the impact of sodium dodecyl sulfate [127]. MALD-MSI is also able to determine the changes of the endogenous components of skin with physiological conditions or disease progression. For instance, the changes of lipid distribution during the maturation of living skin equivalent [128], the role of metallothioneins in melanoma occurrence and progression [129], and the relevance of the molecular features from corneocytes [130] have been successfully identified by MALD-MSI.

As described above, DESI-MSI detecting can be carried out under atmospheric environment. With the help of DESI-MSI, Taudorf et al. [131] evaluated the biodistribution of methotrexate throughout the mid-dermal skin section; D'Alvise et al. [132] demonstrated follicular transport of lidocaine into deeper skin layers. In addition to targeted drug analysis, DESI-MSI also allows one to discriminate and visualize the histologic features of tissue and identify disease progression by imaging associated lipids, proteins and metabolic changes.

Table 1 – Comparison of three types of MSI.

	SIMS	MALDI	DESI
Molecular mass range	100–1500 Da	1000–80,000 Da	100–2000 Da
Sample preparation	No special sample preparation process	Complex sample preparation process, including special slide and matrix spraying	No special sample preparation process and allow detecting under atmospheric pressure
Spatial resolution	400 nm–200 μm	10 μm–200 μm	50 μm–200 μm
Reasons for data distortion	Secondary collision of ions with background	The desorption ability differences of matrix to analytes and the diffusion of analyte in solvent	Solubility difference and displacement of microdroplets on the surface of samples

The differences between SIMS, MALDI-MSI and DESI-MSI are presented in Table 1. SIMS provides high mass resolution, low molecular mass range (*m/z* from 100 to 1500), and good lateral resolution (400 nm to 1–2 μm) [133,134] and does not require specific sample pretreatment or surface modification. However, the fragmentation ions caused by high energy ion clusters, messy noise signals caused by secondary collision of ions with the background, and high demand for the vacuum degree limit SIMS in terms of detectable mass range and sensitivity. Compared with SIMS, the introduction of a matrix reduces the generation of ion fragments and enlarges the range of detectable molecular mass, yet this also brings some trouble. DESI-MSI allows testing under ambient pressure. Unfortunately, the spatial resolution, sensitivity and detectable molecular mass range of DESI-MSI are greatly affected by spray droplet size, solvent composition and spurious contaminants. The solubility difference for analyzed substances and the displacement of microdroplets on a sample surface may cause spatial distortion and quantitative deviation. Meanwhile, according to reports, the measurable molecular mass for DESI-MSI is limited to less than 2000 Da [135].

5. Comparisons

IR and Raman microscopy is used for qualitative and quantitative detection by analyzing the specific wavelength migration, therefore, does not need labeling as for fluorescence microscopy. Both techniques are based on vibrational spectra, many studies have compared IR and Raman microscopy for tissue imaging. Due to the different excitation modes used, these two microscopies show major differences in every aspect. Asymmetric polar moieties have strong IR cross-sections but low Raman cross-sections. Therefore, water may have a strong IR signal and vitally influence the imaging accuracy [136]. The skin' oil CH bands appears around 1700–1800 nm, whereas the water OH bands was proved to centered near 1460 nm and 1920 nm, which is valuable for the detection of the absorption and spreading of moisturizer, but brings trouble to the monitoring of topical substances [137,138]. As for the resolution, it has been reported that the resolution of IR imaging on skin samples is usually limited to several hundreds of microns, but some improved IR microscopies can reach a resolution of 5–10 μm or even higher [139-141]. The acquisition time for Raman microscopes is much longer than that for IR microscope because of the weak Raman signal. However, improvements in equipment hardware can greatly shorten the scanning time. In addition, Raman microscopy provides a much deep penetration depth, richer spatial information, and more accurate qualitative and quantitative results. Raman spectroscopy can be used to locate not only target substances but also image skin structure with submicron resolution, which is difficult to achieve by IR spectroscopy. Therefore, Raman spectroscopy is more commonly used in the field

Table 2 – Comparation of IR spectroscopy, Raman spectroscopy and MSI.

	Infrared spectroscopy	Raman spectroscopy	Mass spectrometry imaging
Energy source	Infrared light source	Ultraviolet to near infrared region	High energy ion beam
Spatial resolution	5–500 μm	Hundreds of microns to sub-microns	Hundreds of microns to sub-microns
Penetration depth	Less than 5 μm	Up to 400 μm	Detecting tissue surface
Requirements for tested substances	Characteristic infrared vibration	Characteristic Raman vibration	Widely suitable for substances with molecular mass from 100 to 80 000 Da
Analytical specificity	Not easy to distinguish substances specifically	Higher specificity and accuracy	Strong substances discrimination ability
Background interference	With serious background interference	Reduced by mathematical calculation, hardware improvement, using of light scavenger, etc.	Mainly comes from matrix or molecular fragment and could be reduced
Major difficulties/ limitation	Background interference and low accuracy	Long acquisition time and data analysis	Pretreatment of samples, no 3D imaging capability

of transdermal imaging. Different from vibration spectrum, MSI directly distinguish target compound by the molecular ion peak, which is more specific. MSI can image hundreds of substances at the same time, but only the substances in the samples' surface can be ionized and transported into the detector. The detailed comparison is presented in Table 2.

6. Conclusion and prospects

The skin a black box for TDDS. A clearer explanation of the transdermal process can help researchers to evaluate the transdermal efficiency, skin pharmacology, and application safety of drugs. The inherent laws concluded from the deeper revealing of transdermal mechanism will contribute to the establish of mathematical models and in silicon dynamic simulation models, significantly reduce the amount of experiments, and deal with the dilemma about cosmetics' animal experiments prohibition. Due to the small molecular mass of most topical substances, the label-free imaging technologies based on the identification of compounds' characteristics is the most ideal imaging technology for transdermal mechanism research.

The label-free imaging technologies described in this review can be used to image endogenous and exogenous substances with a large molecular mass range *in situ* without the need for labeling using macromolecular fluorescent tags. The penetration ability of infrared and Raman microscopies can be even used to maintain the integrity of skin samples. Mass spectrometry imaging has a powerful chemical analysis ability, which can be used to accurately distinguish between hundreds of substances at the same time. The successful application of these technologies helps researchers to further understand the distribution and disposition of topical substances in skin and clarify the role of the skin barrier and skin appendages in the transdermal delivery process. The non-invasive and real-time imaging ability of these technologies provide a solution for *in vivo* dynamic tracking of substances through skin, especially in human body, and help to uncover the skin black box. In the future, the label-free imaging technologies with higher spatial resolution and accuracy, and faster scanning speed, which is expected to achieve satisfactory performance equivalent to confocal microscope, will boost the publish of more surprising results.

However, as we have seen, these techniques are not very prevalent in the field of transdermal mechanism research at present. The reasons for this originate from several aspects: on the one hand, these instruments, as well as corresponding accessories, are not commonly found in laboratories to meet the demand of experiments, let alone modules with high sensitivity and resolution as we have already mentioned. On the other hand, most methods require a strict sample pretreating process or complex mathematical calculation, which brings challenges to researchers. Nonetheless, it is believed that with further study of the transdermal mechanism and the efforts of instrument manufacturers towards the improvement of devices with good performance and low cost, such methods will be recognized more and more by researchers for promoting the progress of relevant research.

Conflicts of interest

We declare that we have no financial and personal relationships with other people or organizations that can inappropriately influence our work.

Supplementary materials

Supplementary material associated with this article can be found, in the online version, at doi:10.1016/j.ajps.2020.07.004.

REFERENCE

[1] Olesen CM, Fuchs CSK, Philipsen PA, Headersdal M, Agner T, Clausen ML. Advancement through epidermis using tape stripping technique and reflectance confocal microscopy. Sci Rep 2019;9:12217.

[2] Briançon S, Bolzinger MA, Chevalier Y. Confocal Raman spectroscopy as a tool to investigate the action of penetration enhancers inside the skin. In: Dragicevic NI, Maibach H, editors. Percutaneous penetration enhancers drug penetration into/through the skin. Berlin, Heidelberg: Springer; 2017. p. 229–46.

[3] Keurentjes AJ, Maibach HI. Percutaneous penetration of drugs applied in transdermal delivery systems: an *in vivo* based approach for evaluating computer generated penetration models. Regul Toxicol Pharmacol 2019;108:104428.

[4] Niu J, Chu Y, Huang YF, Chong YS, Jiang ZH, Mao ZW, et al. Transdermal gene delivery by functional peptide conjugated cationic gold nanoparticle reverses the progression and metastasis of cutaneous melanomaTransdermal gene delivery by functional peptide conjugated cationic gold nanoparticle reverses the progression and metastasis of cutaneous melanoma. ACS Appl Mater Interfaces 2017;9(11):9388–401.

[5] Peng LH, Xu SY, Shan YH, Wei W, Liu S, Zhang CZ, et al. Sequential release of salidroside and paeonol from a nanosphere-hydrogel system inhibits ultraviolet B-induced melanogenesis in guinea pig skin. Int J Nanomed 2014;9:1897–908.

[6] Hu Y, Wu YY, Xia XJ, Wu Z, Liang WQ, Gao JQ. Development of drug-in-adhesive transdermal patch for alpha-asarone and *in vivo* pharmacokinetics and efficacy evaluation. Drug Deliv 2011;18(1):84–9.

[7] Paudel KS, Milewski M, Swadley CL, Brogden NK, Ghosh P, Stinchcomb AL. Challenges and opportunities in dermal/transdermal delivery. Ther Deliv 2010;1(1):109–31.

[8] Yang S, Wang R, Wan G, Wu ZM, Guo SJ, Dai XX, et al. A Multiscale study on the penetration enhancement mechanism of menthol to osthole. J Chem Inf Model 2016;56(11):2234–42.

[9] Todosijević MN, Brezesinski G, Savic SD, Neubert RHH. Sucrose esters as biocompatible surfactants for penetration enhancement: an insight into the mechanism of penetration enhancement studied using stratum corneum model lipids and Langmuir monolayers. Eur J Pharm Sci 2017;99:161–72.

[10] Niu XQ, Zhang DP, Bian Q, Feng XF, Li H, Rao YF, et al. Mechanism investigation of ethosomes transdermal permeation. Int J Pharm X 2019;1:100027.

[11] Barbero AM, Frasch HF. Effect of stratum corneum heterogeneity, anisotropy, asymmetry and follicular

pathway on transdermal penetration. J Control Release 2017;260:234–46.
[12] Doucet J, Potter A, Baltenneck C, Domanov YA. Micron-scale assessment of molecular lipid organization in human stratum corneum using microprobe X-ray diffraction. J Lipid Res 2014;55(11):2380–8.
[13] Wertz PW. Current understanding of skin biology pertinent to skin penetration: skin biochemistry. Skin Pharmacol Physiol 2013;26(4–6):217–26.
[14] Choe C, Schleusener J, Lademann J, Darvin ME. Keratin-water-NMF interaction as a three-layer model in the human stratum corneum using *in vivo* confocal Raman microscopy. Sci Rep 2017;7(1):15900.
[15] Pathan I, Setty C. Chemical penetration enhancers for transdermal drug delivery systems. Trop J Pharm Res 2009;8(2):173–9.
[16] Lefcoski S, Kew K, Reece S, Torres MJ, Parks J, Reece S, et al. Anatomical-molecular distribution of ephrinA1 in infarcted mouse heart using MALDI mass spectrometry imaging. J Am Soc Mass Spectrom 2018;29(3):527–34.
[17] Choe C, Lademann J, Darvin ME. A depth-dependent profile of the lipid conformation and lateral packing order of the stratum corneum *in vivo* measured using Raman microscopy. Analyst 2016;141(6):1981–7.
[18] Grubauer G, Feingold KR, Harris RM, Elias PM. Lipid content and lipid type as determinants of the epidermal permeability barrier. J Lipid Res 1989;30(1):89–96.
[19] Masukawa Y, Narita H, Shimizu E, Kondo N, Sugai Y, Oba T, et al. Characterization of overall ceramide species in human stratum corneum. J Lipid Res 2008;49(7):1466–76.
[20] Chen X, Gregoire S, Formanek F, Galey JB, Rigneault H. Quantitative 3D molecular cutaneous absorption in human skin using label free nonlinear microscopy. J Control Release 2015;200:78–86.
[21] David N. Prodrug strategies for enhancing the percutaneous absorption of drugs. Molecules 2014;19(12):20780–807.
[22] Anissimov YG, Jepps OG, Dancik Y, Roberts MS. Mathematical and pharmacokinetic modelling of epidermal and dermal transport processes. Adv Drug Deliv Rev 2013;65(2):169–90.
[23] Selzer D, Neumann D, Schaefer UF. Mathematical models for dermal drug absorption. Expert Opin Drug Metab Toxicol 2015;11(10):1567–83.
[24] Anissimov YG, Watkinson A. Modelling skin penetration using the laplace transform technique. Skin Pharmacol Physiol 2013;26(4–6):286–94.
[25] Covi-Schwarz J, Klang V, Valenta C. ATR-FTIR spectroscopy and the skin barrier: evaluation of penetration-enhancement effects. Percutaneous penetration enhancers drug penetration into/through the skin. Berlin Heidelberg: Springer-Verlag; 2017. p. 247–54.
[26] Boncheva M, Tay FH, Kazarian SG. Application of attenuated total reflection Fourier transform infrared imaging and tape-stripping to investigate the three-dimensional distribution of exogenous chemicals and the molecular organization in Stratum corneum. J Biomed Opt 2008;13(6):064009.
[27] Garidel P. Insights in the biochemical composition of skin as investigated by micro infrared spectroscopic imaging. Phys Chem Chem Phys 2003;5(12):2673–9.
[28] Wang F, Cao S, Yan R, Wang Z, Wang D, Yang H. Selectivity/specificity improvement strategies in surface-enhanced Raman spectroscopy analysis. Sensors 2017;17(11):2689.
[29] Cheng J, Xie XS. Coherent anti-stokes Raman scattering microscopy: instrumentation, theory, and applications. J Phys Chem B 2004;108(3):827–40.
[30] Tipping WJ, Lee M, Serrels A, Brunton VG, Hulme AN. Stimulated Raman scattering microscopy: an emerging tool for drug discovery. Chem Soc Rev 2016;45(8):2075–89.
[31] Konorov SO, Blades MW, Turner RFB. Non-resonant background suppression by destructive interference in coherent anti-Stokes Raman scattering spectroscopy. Opt Express 2011;19(27):25925–34.
[32] Choi DS, Kim CH, Lee T, Nah S, Rhee H, Cho M. Vibrational spectroscopy and imaging with non-resonant coherent anti-stokes Raman scattering: double stimulated Raman scattering scheme. Opt Express 2019;27(16):23558–75.
[33] Benalcazar WA, Boppart SA. Nonlinear interferometric vibrational imaging for fast label-free visualization of molecular domains in skin. Anal Bioanal Chem 2011;400(9):2817 25.
[34] Sarri B, Chen XQ, Canonge R, Gregoire S, Formanek F, Galey JB, et al. *In vivo* quantitative molecular absorption of glycerol in human skin using coherent anti-Stokes Raman scattering (CARS) and two-photon auto-fluorescence. J Control Release 2019;308:190–6.
[35] Benalcazar WA, Boppart SA. Nonlinear interferometric vibrational imaging for fast label-free visualization of molecular domains in skin. Anal Bioanal Chem 2011;400(9):2817 5.
[36] Sultan M, Schulz MH, Richard H, Magen A, Klingenhoff A, Scherf M, et al. A global view of gene activity and alternative splicing by deep sequencing of the human transcriptome. Science 2008;321(5891):956–60.
[37] Cheng JX, Xie XS. Vibrational spectroscopic imaging of living systems: an emerging platform for biology and medicine. Science 2015;350(6264):aaa8870.
[38] Wei L, Hu FH, Chen ZX, Shen YH, Zhang LY, Min W. Live-cell bioorthogonal chemical imaging: stimulated Raman scattering microscopy of vibrational probes. Acc Chem Res 2016;49(8):1494–502.
[39] Ashtikar MA, Verma DD, Fahr A. Confocal microscopy for visualization of skin penetration. In: Dragicevic NI, Maibach H, editors. Percutaneous penetration enhancers drug penetration into/through the skin. Berlin, Heidelberg: Springe; 2017. p. 255–81.
[40] Zhang D, Wang P, Slipchenko MN, Cheng JX. Fast vibrational imaging of single cells and tissues by stimulated Raman scattering microscopy. Acc Chem Res 2014;47(8):2282–90.
[41] Berto P, Andresen ER, Rigneault H. Background-free stimulated Raman spectroscopy and microscopy. Phys Rev Lett 2014;112(5):053905.
[42] Fu D, Lu FK, Zhang X, Freudiger C, Pernik DR, Holtom G, et al. Quantitative chemical imaging with multiplex stimulated Raman scattering microscopy. J Am Chem Soc 2012;134(8):3623–6.
[43] Touboul D, Kollmer F, Niehuis E, Brunelle A, Laprevote O. Improvement of biological time-of-flight-secondary ion mass spectrometry imaging with a bismuth cluster ion source. J Am Soc Mass Spectrom 2005;16(10):1608–18.
[44] Nakano S, Yokoyama Y, Aoyagi S, Himi N, Fletcher JS, Lockyer NP, et al. Evaluation of biomolecular distributions in rat brain tissues by means of ToF-SIMS using a continuous beam of Ar clusters. Biointerphases 2016;11(2):02A307.
[45] Ishikawa K, Okamoto M, Aoyagi S. Structural analysis of the outermost hair surface using TOF-SIMS with gas cluster ion beam sputtering. Biointerphases 2016; 11(2):02A315.
[46] Mohammadi AS, Phan NTN, Fletcher JS, Ewing AG. Intact lipid imaging of mouse brain samples: MALDI, nanoparticle-laser desorption ionization, and 40 keV argon cluster secondary ion mass spectrometry. Anal Bioanal Chem 2016;408(24):6857–68.

[47] Hsu CC, Chou PT, Zare RN. Imaging of proteins in tissue samples using nanospray desorption electrospray ionization mass spectrometry. Anal Chem 2015;87(22):11171–5.
[48] Yang J, Caprioli RM. Matrix pre-coated targets for high throughput MALDI imaging of proteins. J Mass Spectrom 2014;49(5):417–22.
[49] Vickerman JC. Molecular imaging and depth profiling by mass spectrometry-SIMS, MALDI or DESI. Analyst 2011;136(11):2199.
[50] Barry JA, Groseclose MR, Robichaud G, Castellino S, Muddiman DC. Assessing drug and metabolite detection in liver tissue by UV-MALDI and IR-MALDESI mass spectrometry imaging coupled to FT-ICR MS. Int J Mass Spectrom 2015;377:448–55.
[51] De Macedo CS, Anderson DM, Schey KL. MALDI (matrix assisted laser desorption ionization) imaging mass spectrometry (IMS) of skin: aspects of sample preparation. Talanta 2017;174:325–35.
[52] Francese S, Bradshaw R, Flinders B, Mitchell C, Bleay S, Cicero L, et al. Curcumin: a multipurpose matrix for MALDI mass spectrometry imaging applications. Anal Chem 2013;85(10):5240–8.
[53] Enthaler B, Pruns JK, Wessel S, Rapp C, Fischer M, Wittern KP. Improved sample preparation for MALDI–MSI of endogenous compounds in skin tissue sections and mapping of exogenous active compounds subsequent to ex-vivo skin penetration. Anal Bioanal Chem 2012;402(3):1159–67.
[54] Sun CL, Li ZC, Ma CX, Zang QC, Li JS, Liu W, et al. Acetone immersion enhanced MALDI-MS imaging of small molecule metabolites in biological tissues. J Pharm Biomed Anal 2019;176:112797.
[55] Yang H, Ji W, Guan M, Li SL, Zhang YY, Zhao ZW, et al. Organic washes of tissue sections for comprehensive analysis of small molecule metabolites by MALDI MS imaging of rat brain following status epilepticus. Metabolomics 2018;14(4):50.
[56] Mansour RSH, Sallam AA, Hamdan II, Khalil EA, Yousef I. Elucidation of penetration enhancement mechanism of Emu oil using FTIR microspectroscopy at EMIRA laboratory of SESAME synchrotron. Spectrochim Acta A 2017; 185:1–10.
[57] Zhang QH, Saad P, Mao GR, Walters RM, Correa MCM, Mendelsohn R, et al. Infrared spectroscopic imaging tracks lateral distribution in human stratum corneum. Pharm Res 2014;31(10):2762–73.
[58] Jiang J, Boese M, Turner P, Wang RKK. Penetration kinetics of dimethyl sulphoxide and glycerol in dynamic optical clearing of porcine skin tissue *in vitro* studied by Fourier transform infrared spectroscopic imaging. J Biomed Opt 2008;13(2):021105.
[59] Tfaili S, Gobinet C, Josse G, Angiboust JF, Baillet A, Manfait M, et al. Vibrational spectroscopies for the analysis of cutaneous permeation: experimental limiting factors identified in the case of caffeine penetration. Anal Bioanal Chem 2012;405(4):1325–32.
[60] Mendelsohn R, Chen HC, Rerek ME, Moore DJ. Infrared microspectroscopic imaging maps the spatial distribution of exogenous molecules in skin. J Biomed Opt 2003;8(2):185–90.
[61] Andrew Chan AKL, Kazarian SG. Chemical imaging of the stratum corneum under controlled humidity with the attenuated total reflection fourier transform infrared spectroscopy method. J Biomed Opt 2007;12(4):044010.
[62] Binder L, Kulovits EM, Petz R, Ruthofer J, Baurecht D, Klang V, et al. Penetration monitoring of drugs and additives by ATR-FTIR spectroscopy/tape stripping and confocal Raman spectroscopy-a comparative study. J Pharm Biomed Anal 2018;130:214–23.
[63] Andanson JM, Hadgraft J, Kazarian SG. In situ permeation study of drug through the stratum corneum using attenuated total reflection Fourier transform infrared spectroscopic imaging. J Biomed Opt 2009;14(3):034011.
[64] Schwarz JC, Pagitsch E, Valenta C. Comparison of ATR-FTIR spectra of porcine vaginal and buccal mucosa with ear skin and penetration analysis of drug and vehicle components into pig ear. Eur J Pharm Sci 2013;50(5):595–600.
[65] Goh CF, Craig DQM, Hadgraft J, Lane ME. The application of ATR-FTIR spectroscopy and multivariate data analysis to study drug crystallisation in the stratum corneum. J Pharm Biomed Anal 2017;111:16–25.
[66] Hoppel M, Baurecht D, Holper E, Mahrhauser D, Valenta C. Validation of the combined ATR-FTIR/tape stripping technique for monitoring the distribution of surfactants in the stratum corneum. Int J Pharm 2014;472(1–2):88–93.
[67] Wolf M, Halper M, Pribyl R, Baurecht D, Valenta C. Distribution of phospholipid based formulations in the skin investigated by combined ATR-FTIR and tape stripping experiments. Int J Pharm 2017;519(1–2):198–205.
[68] Hoppel M, Holper E, Baurecht D, Valenta C. Monitoring the distribution of surfactants in the stratum corneum by combined ATR-FTIR and tape-stripping experiments. Skin Pharmacol Physiol 2015;28(3):167–75.
[69] Nawaz A, Wong TW. Quantitative characterization of chitosan in the skin by Fourier-transform infrared spectroscopic imaging and ninhydrin assay: application in transdermal sciences. J Microsc 2016;263(1):34–42.
[70] Cozzi AC, Perugini P, Gourion-Arsiquaud S. Comparative behavior between sunscreens based on free or encapsulated UV filters in term of skin penetration, retention and photo-stability. Eur J Pharm Sci 2018;121:309–18.
[71] Higo N, Naik A, Bommannan DB, Potts RO, Guy RH. Validation of reflectance infrared spectroscopy as a quantitative method to measure percutaneous absorption *in vivo*. Pharm Res 1993;10(10):1500–6.
[72] Alberti I, Kalia YN, Naik A, Bonny JD, Guy RH. Effect of ethanol and isopropyl myristate on the availability of topical terbinafine in human stratum corneum, *in vivo*. Int J Pharm 2001;219(1):11–19.
[73] Kazarian SG, Chan KLA. Applications of ATR-FTIR spectroscopic imaging to biomedical samples. Biochim Biophys Acta Biomembr 2006;1758(7):858–67.
[74] Mao G, Flach CR, Mendelsohn R, Walters RM. Imaging the distribution of sodium dodecyl sulfate in skin by confocal Raman and infrared microspectroscopy. Pharm Res 2012;29(8):2189–201.
[75] Tfayli A, Piot O, Pitre F, Manfait M. Follow-up of drug permeation through excised human skin with confocal Raman microspectroscopy. Eur Biophys J 2007; 36(8):1049–58.
[76] Bonnist EYM, Gorce JP, Mackay C, Pendlington RU, Pudney PDA. Measuring the penetration of a skin sensitizer and its delivery vehicles simultaneously with confocal Raman spectroscopy. Skin Pharmacol Physiol 2011;24(5):274–83.
[77] Essendoubi M, Gobinet C, Reynaud R, Angiboust JF, Manfait M, Piot O. Human skin penetration of hyaluronic acid of different molecular weights as probed by Raman spectroscopy. Skin Res Technol 2016;22(1):55–62.
[78] Förster M, Bolzinger MA, Ach D, Montagnac G, Briancon S. Ingredients tracking of cosmetic formulations in the skin: a confocal Raman microscopy investigation. Pharm Res 2011;28(4):858–72.

[79] Choe C, Lademann J, Darvin ME. Analysis of human and porcine skin *in vivo/ex vivo* for penetration of selected oils by confocal Raman microscopy. Skin Pharmacol Physiol 2015;28(6):318–30.
[80] Mujica Ascencio S, Choe CS, Meinke MC, Muller RH, Maksimov GV, Wigger-Alberti W, et al. Confocal Raman microscopy and multivariate statistical analysis for determination of different penetration abilities of caffeine and propylene glycol applied simultaneously in a mixture on porcine skin *ex vivo*. J Pharm Biomed Anal 2016;104:51–8.
[81] Pyatski Y, Zhang QH, Mendelsohn R, Flach CR. Effects of permeation enhancers on flufenamic acid delivery in *ex vivo* human skin by confocal Raman microscopy. Int J Pharm 2016;505(1–2):319–28.
[82] Bakonyi M, Gácsi A, Kovács A, Szucs MB, Berko S, Csanyi E. Following-up skin penetration of lidocaine from different vehicles by Raman spectroscopic mapping. J Pharm Biomed Anal 2018;154:1–6.
[83] Darvin ME, Thiede G, Ascencio SM, Schanzer S, Richter H, Vinzon SE, et al. *In vivo/ex vivo* targeting of langerhans cells after topical application of the immune response modifier TMX-202: confocal Raman microscopy and histology analysis. J Biomed Opt 2016;21(5):055004.
[84] Franzen L, Mathes C, Hansen S, Windbergs M. Advanced chemical imaging and comparison of human and porcine hair follicles for drug delivery by confocal Raman microscopy. Biomed Opt 2012;18(6):061210.
[85] Mélot M, Pudney PDA, Williamson AM, Caspers PJ, Van Der Pol A, Puppels GJ. Studying the effectiveness of penetration enhancers to deliver retinol through the stratum corneum by *in vivo* confocal Raman spectroscopy. J Control Release 2009;138(1):32–9.
[86] Laing S, Bielfeldt S, Wilhelm KP, Obst J. Confocal Raman spectroscopy as a tool to measure the prevention of skin penetration by a specifically designed topical medical device. Skin Res Technol 2019;25(4):578–86.
[87] Dos Santos L, Téllez SCA, Sousa MPJ, Azoia NG, Cavaco-Paulo AM, Martin AA, et al. *In vivo* confocal Raman spectroscopy and molecular dynamics analysis of penetration of retinyl acetate into stratum corneum. Spectrochim Acta A 2017;174:279–85.
[88] Egawa M, Sato Y. *In vivo* evaluation of two forms of urea in the skin by Raman spectroscopy after application of urea-containing cream. Skin Res Technol 2014;21(3):259–64.
[89] Tippavajhala VK, de Oliveira Mendes T, Martin AA. *In vivo* human skin penetration study of sunscreens by confocal Raman spectroscopy. AAPS PharmSciTech 2018;19(2):753–60.
[90] Bi YL, Yang C, Chen YG, Yan S, Yang G, Wu YZ, et al. Near-resonance enhanced label-free stimulated Raman scattering microscopy with spatial resolution near 130 nm. Light Sci Appl 2018;7(1):81.
[91] Saar BG, Contreras-rojas LR, Xie XS, Guy RH. Imaging drug delivery to skin with stimulated Raman scattering microscopy. Mol Pharm 2011;8(3):969–75.
[92] Belsey NA, Garrett NL, Contreras-Rojas LR, Pickup-Gerlaugh AJ, Price GJ, Moger J, et al. Evaluation of drug delivery to intact and porated skin by coherent Raman scattering and fluorescence microscopies. J Control Release 2014;174:37–42.
[93] Drutis DM, Hancewicz TM, Pashkovski E, Feng L, Mihalov D, Holtom G, et al. Three-dimensional chemical imaging of skin using stimulated Raman scattering microscopy. J Biomed Opt 2014;19(11):111604.
[94] Garrett NL, Singh B, Jones A, Moger J. Imaging microscopic distribution of antifungal agents in dandruff treatments with stimulated Raman scattering microscopy. J Biomed Opt 2017;22(6):066003.
[95] Perticaroli S, Yeomans DJ, Wireko FC. Translating chemometric analysis into physiological insights from *in vivo* confocal Raman spectroscopy of the human stratum corneum. Biochim Biophys Acta Biomembr 2019;1861(2):403–9.
[96] Tippavajhala VK, Mendes TO, Martin AA. *In vivo* human skin penetration study of sunscreens by confocal Raman spectroscopy. AAPS PharmSciTech 2018;19(2):753–60.
[97] Miloudi L., Bonnier F., Tfayli A., Yvergnaux F., Byrne H.J., Chourpa I., et al. Confocal Raman spectroscopic imaging for *in vitro* monitoring of active ingredient penetration and distribution in reconstructed human epidermis mode. J Biophotonics 2017: e201700221.
[98] Franzen L, Anderski J, Windbergs M. Quantitative detection of caffeine in human skin by confocal Raman spectroscopy-a systematic *in vitro* validation study. J Pharm Biomed Anal 2015;95:110–16.
[99] Alonso C, Carrer V, Barba C, Coderch L. Caffeine delivery in porcine skin: a confocal Raman study. Arch Dermatol Res 2018;310(8):657–64.
[100] Choe C, Ri J, Schleusener J, Lademann J, Darvin ME. The non-homogenous distribution and aggregation of carotenoids in the stratum corneum correlates with the organization of intercellular lipids *in vivo*. Exp Dermatol 2019;28(11):1237–43.
[101] Schleusener J, Lademann J, Darvin ME. Depth-dependent autofluorescence photobleaching using 325, 473, 633, and 785 nm of porcine ear skin *ex vivo*. J Biomed Opt 2017;22(9):091503.
[102] Trotta M, Rhodes LE, Sage E. Shine on you crazy books: the comprehensive series in photochemical & photobiological sciences. Photoch Photobio Sci 2016;15(1):8–9.
[103] Wang H, Zhao J, Lee AMD, Lui H, Zeng HS. Improving skin Raman spectral quality by fluorescence photobleaching. Photodiagnosis Photodyn Ther 2012;9(4):299–302.
[104] Ferulova I, Lihachev A, Spigulis J. Photobleaching effects on *in vivo* skin autofluorescence lifetime. J Biomed Opt 2015;20(5):051031.
[105] Darvin ME, Schleusener J, Parenz F, Seidel O, Krafft C, Popp J, et al. Confocal Raman microscopy combined with optical clearing for identification of inks in multicolored tattooed skin *in vivo*. Analyst 2018;143(20):4990–9.
[106] Lee SH, Jun SH, Yeom J, Park SG, Lee CK, Kang NG. Optical clearing agent reduces scattering of light by the stratum corneum and modulates the physical properties of coenocytes via hydration. Skin Res Technol 2018;24(3):371–8.
[107] Liu P, Huang YY, Guo ZY, Wang JP, Zhuang ZF, Liu SH. Discrimination of dimethyl sulphoxide diffusion coefficient in the process of optical clearing by confocal micro-Raman spectroscopy. J Biomed Opt 2013;18(2):020507.
[108] Sdobnov AY, Tuchin VV, Lademann J, Darvin ME. Confocal Raman microscopy supported by optical clearing treatment of the skin-influence on collagen hydration. J Phys D 2017;50(28):285401.
[109] Zimmerley M, Mcclure RA, Choi B, Potma EO. Following dimethyl sulfoxide skin optical clearing dynamics with quantitative nonlinear multimodal microscopy. Appl Opt 2009;48(10):79–87.
[110] Sdobnov AY, Darvin ME, Schleusener J, Lademann J, Tuchin VV. Hydrogen bound water profiles in the skin influenced by optical clearing molecular agents-quantitative analysis using confocal Raman microscopy. J Biophotonics 2018;12(5):e201800283.
[111] Sdobnov AY, Lademann J, Darvin ME, Tuchin VV. Methods for optical skin clearing in molecular optical imaging in dermatology. Biochemistry 2019;84(S1):144–58.
[112] Holmes AM, Scurr DJ, Heylings JR, Wan KW, Moss GP. Dendrimer pre-treatment enhances the skin permeation of

chlorhexidine digluconate: characterisation by *in vitro* percutaneous absorption studies and time-of-flight secondary ion mass spectrometry. Eur J Pharm Sci 2017;104:90–101.
[113] Monteiro-Riviere NA, Wiench K, Landsiedel R, Schulte S, Inman AO, Riviere JE. Safety evaluation of sunscreen formulations containing titanium dioxide and zinc oxide nanoparticles in UVB sunburned skin: an *in vitro* and *in vivo* study. Toxicol Sci 2011;123(1):264–80.
[114] Čižinauskas V, Elie N, Brunelle A, Briedis V. Skin penetration enhancement by natural oils for dihydroquercetin delivery. Molecules 2017;22(9):1536.
[115] Starr NJ, Hamid KA, Wibawa J, Marlow I, Bell M, Perez-Garcia L, et al. Enhanced vitamin C skin permeation from supramolecular hydrogels, illustrated using *in situ* ToF-SIMS 3D chemical profiling. Int J Pharm 2019;563:21–9.
[116] Kijima S, Todo H, Matsumoto Y, Masaki R, Kadhum WR, Sugibayashi K. A useful technique using imaging mass spectrometry for detecting the skin distribution of topically applied lidocaine. J Drug Deliv Sci Technol 2016;33:157–63.
[117] Al-Mayahy MH, Sabri AH, Rutland CS, Holmes A, McKenna J, Marlow M, et al. Insight into imiquimod skin permeation and increased delivery using microneedle pre-treatment. J Pharm Biomed Anal 2019;139:33–43.
[118] Sjövall P, Greve TM, Clausen SK, Moller K, Eirefelt S, Johansson B, et al. Imaging of distribution of topically applied drug molecules in mouse skin by combination of TOF-SIMS and SEM. Anal Chem 2014;55(5):956–74.
[119] Sjovall P, Skedung L, Gregoire S, Biganska O, Clement F, Luengo GS. Imaging the distribution of skin lipids and topically applied compounds in human skin using mass spectrometry. Sci Rep 2018;8:16683.
[120] Bonnel D, Legouffe R, Eriksson AH, Mortensen RW, Pamelard F, Stauber J, et al. MALDI imaging facilitates new topical drug development process by determining quantitative skin distribution profiles. Anal Bioanal Chem 2018;410(2):2815 28.
[121] Hendel KK, Bagger C, Olesen UH, Janfelt C, Hansen SH, Haedersdal M, et al. Fractional laser-assisted topical delivery of bleomycin quantified by LC-MS and visualized by MALDI mass spectrometry imaging. Drug Deliv 2019;26(1):244–51.
[122] Avery JL, McEwen A, Flinders B, Francese S, Clench MR. Matrix-assisted laser desorption mass spectrometry imaging for the examination of imipramine absorption by Straticell-RHE-EPI/001 an artificial model of the human epidermis. Xenobiotica 2011;41(8):735–42.
[123] Harvey A, Cole LM, Day R, Bartlett M, Warwick J, Bojar R, et al. MALDI-MSI for the analysis of a 3D tissue-engineered psoriatic skin model. Proteomics 2016;16(11–12):1718–25.
[124] Bunch J, Clench MR, Richards DS. Determination of pharmaceutical compounds in skin by imaging matrix-assisted laser desorption/ionisation mass spectrometry. Rapid Commun Mass Spectrom 2004;18(24):3051–60.
[125] Marxen E, Jin L, Jacobsen J, Janfelt C, Hyrup B, Nicolazzo JA. Effect of permeation enhancers on the buccal permeability of nicotine: *ex vivo* transport studies complemented by MALDI MS imaging. Pharm Res 2018;35(3):70.
[126] Marxen E, Jacobsen J, Hyrup B, Janfelt C. Permeability barriers for nicotine and mannitol in porcine buccal mucosa studied by high-resolution MALDI mass spectrometry imaging. Mol Pharm 2018;15(2):519–26.
[127] Hansen SE, Marxen E, Janfelt C, Jacobsen J. Buccal delivery of small molecules -impact of levulinic acid, oleic acid, sodium dodecyl sulfate and hypotonicity on *ex vivo* permeability and spatial distribution in mucosa. J Pharm Biomed Anal 2018;133:250–7.
[128] Mitchell CA, Long H, Donaldson M, Francese S, Clench MR. Lipid changes within the epidermis of living skin equivalents observed across a time-course by MALDI-MS imaging and profiling. Lipids Health Dis 2015; 14(1):84.
[129] Vanickova L, Guran R, Kollár S, Emri G, Krizkova S, Do T, et al. Mass spectrometric imaging of cysteine rich proteins in human skin. Int J Biol Macromol 2019;125:270–7.
[130] Hochart G, Bonnel D, Stauber J, Stamatas GN. Biomarker mapping on skin tape strips using MALDI mass spectrometry imaging. J Am Soc Mass Spectrom 2019;30(10):2082–91.
[131] Taudorf EH, Lerche CM, Vissing AC, Philipsen PA, Hannibal J, D'Alvise J, et al. Topically applied methotrexate is rapidly delivered into skin by fractional laser ablation. Expert Opin Drug Deliv 2015;12(7):1059–69.
[132] D'Alvise J, Mortensen R, Hansen SH, Janfelt C. Detection of follicular transport of lidocaine and metabolism in adipose tissue in pig ear skin by DESI mass spectrometry imaging. Anal Bioanal Chem 2014;406(15):3735–42.
[133] Desbenoit N, Walch A, Spengler B, Brunelle A, Rompp A. Correlative mass spectrometry imaging, applying time-of-flight secondary ion mass spectrometry and atmospheric pressure matrix-assisted laser desorption/ionization to a single tissue section. Rapid Commun Mass Spectrom 2018;32(2):159–66.
[134] Judd AM, Scurr DJ, Heylings JR, Wan KW, Moss GP. Distribution and visualisation of chlorhexidine within the skin using ToF-SIMS: a potential platform for the design of more efficacious skin antiseptic formulations. Pharm Res 2013;30(7):1896–905.
[135] Qin L, Zhang YW, Liu YQ, He HX, Han MM, Li YY, et al. Recent advances in matrix-assisted laser desorption/ionisation mass spectrometry imaging (MALDI-MSI) for *in situ* analysis of endogenous molecules in plants. Phytochem Anal 2018;29(4):351–64.
[136] Ali SM, Bonnier F, Lambkin H, Flynn K, McDonagh V, Healy C, et al. A comparison of Raman, FTIR and ATR-FTIR micro spectroscopy for imaging human skin tissue sections. Anal Methods 2013;5(9):2281–91.
[137] Egawa M, Yanai M, Kikuchi K, Masuda Y. Extended range near-infrared imaging of water and oil in facial skin. Appl Spectrosc 2011;65(8):924–30.
[138] Arimoto H, Yanai M, Egawa M. Analysis of absorption and spreading of moisturizer on the microscopic region of the skin surface with near-infrared imaging. Skin Res Technol 2016;22(4):505–12.
[139] Kerr JL, Baldwin DS, Tobin MJ, et al. High spatial resolution infrared micro-spectroscopy reveals the mechanism of leaf lignin decomposition by aquatic fungi. PLoS ONE 2013;8(4):e60857.
[140] Großerueschkamp F, Bracht T, Diehl HC, Kuepper C, Ahrens M, Kallenbach-Thieltges A, et al. Spatial and molecular resolution of diffuse malignant mesothelioma heterogeneity by integrating label-free FTIR imaging, laser capture microdissection and proteomics. Sci Rep 2017;7(1):44829.
[141] Kimber JA, Foreman L, Turner B, Rich P, Kazarian SG. FTIR spectroscopic imaging and mapping with correcting lenses for studies of biological cells and tissues. Faraday Discuss 2016;187:69–85.